2012 IEEE/SICE International Symposium on System Integration (SII)
Kyushu University, Fukuoka, Japan
December 16-18, 2012

Robot-assisted RF Ablation with Interactive Planning and Mixed Reality Guidance

Rong Wen, Chin-Boon Chng, Chee-Kong Chui*, *Member, IEEE*, Kah-Bin Lim, Sim-Heng Ong and Stephen Kin-Yong Chang

***Abstract*—Radiofrequency (RF) ablation delivered through interventional procedure is a good alternative to hepatic resection or liver transplant for treatment of liver tumor. However, inefficient RF needle navigation and limited thermal ablation region challenge surgeons' manipulations. This paper presents robot-assisted RF ablation system for liver tumor treatment with interactive planning and mixed reality guidance. Interactive planning involves ablation model planning and surgeon's supervisory feedback via projector-based augmented reality (AR). The preoperatively defined surgical planning data is visualized directly on the patient body through the AR display, supplying information of insertion points, ablation points as well as preplanned trajectories, before execution by robot. The needle's spatial insertion is intraoperatively navigated by stereoscopic tracking and simulated in a model based virtual environment comprising anatomic and RF needle models. The robotic execution benefited from improved accuracy on needle's tip tracking and model based simulation. *Ex vivo* model and *in vivo* animal studies were conducted to validate and assess the performance of proposed mechanism. This solution is promising in overcoming current technological limitations and practical constraints of precise transcutaneous ablation therapy.**

I. Introduction

Hepatic resection or liver transplantation offers greatest potential for curing the patient with primary and metastatic liver tumors [1]. However, only 10–20% of the patients with liver tumors are suitable for these procedures due to surgical constraints such as tumor size, tumor location as well as poor general health and potential impacts on functional reserve [2]. Among various ablative therapies which are currently available to treat patients with unresectable liver malignancies, radiofrequency ablation (RFA) is widely used because of its safety, ease of application and thermal ablative consistency [2]. Radiofrequency generator produces high-frequency (200—1200 HZ) heat on the tip of a needle electrode to create a region of necrosis with a result of localized cellular death.

Although RFA is an effective approach for treatment of liver metastatic, it faces the challenge of inadequate vision information for RF needle navigation and a tremendous handicap on dexterity of the surgeon [1].

Current practice for transcutaneous RF ablation involves a series of imaging and manual insertion based on the judgment of radiologists or surgeons. This method is tedious and often subject to uncertainties especially in the case of large tumors where multiple needle insertions are required to destroy the entire tumor. Ultrasound (US) image-guided surgery is widely used as an intraoperative modality [3]. While experienced surgeons may perform ablation therapy using real time ultrasound image guidance, this method has its disadvantages including the lack of depth perception and the creation of transient hyperechoic zones due to the microbubbles in ablated tissue, complicating subsequent insertions of the electrode at the target sites. In this regard, surgical robot with its heightened speed, accuracy, and consistency is an appropriate candidate for the execution of preplanned needle trajectory in RFA.

A variety of surgical robots and tracked navigation systems have been investigated to assist image guided with free hand and accurate insertion [4], [5]. Coupled with intuitive computer assisted visualization modules for surgical planning, surgeons can better achieve their treatment objectives. In our previous study [4], we described a manipulator that was specialized in the execution of the overlapping RFA technique, considering both kinematics and clinical requirements. Besides, a voxel-growing algorithm was proposed to automatically produce ablation points for robotic execution.

In recent years, advances in imaging techniques assist surgeons to identify the preoperatively defined surgical planning data in surgery. Nakamoto *et al*. [3] described an ultrasound system that aims to achieve augmented reality (AR) visualization during laparoscopic surgery in which a calibration is required for intraoperative magnetic distortion. In order to enhance intraoperative US images, information of computed tomography (CT) images are integrated. To avoid switching view focus between the monitor and the patient during the procedure of needle insertion, an image overlay system with semi-transparent mirror was presented by Fichtinger *et al* [5]. In addition, monitor-based AR display has been tested in the minimally invasive surgeries which

This work was supported in part by the National University of Singapore (NUS), Singapore under Grants R-265-000-270-112 and R-265-000-270-133. *Asterisk indicates corresponding author*.

*Chee-Kong Chui is with Department of Mechanical Engineering, NUS. (fax: (65) 6779 1459, e-mail: mpecck@nus.edu.sg). R. Wen, C.-B. Chng, and K.-B. Lim are also with the Department of Mechanical Engineering (e-mail:g0801390@nus.edu.sg; mpeccb@nus.edu.sg; mpelimkb@nus.edu.sg). S.-H. Ong is with the Department of Electrical & Computer Engineering (e-mail: eleongsh@nus.edu.sg). S. K.-Y. Chang is with Department of Surgery, National University Hospital, Singapore (e-mail: cfscky@nus.edu.sg).

enable surgeons to view hidden critical structures and tissues beneath the real scene from a fixed monitor.

II. System Overview

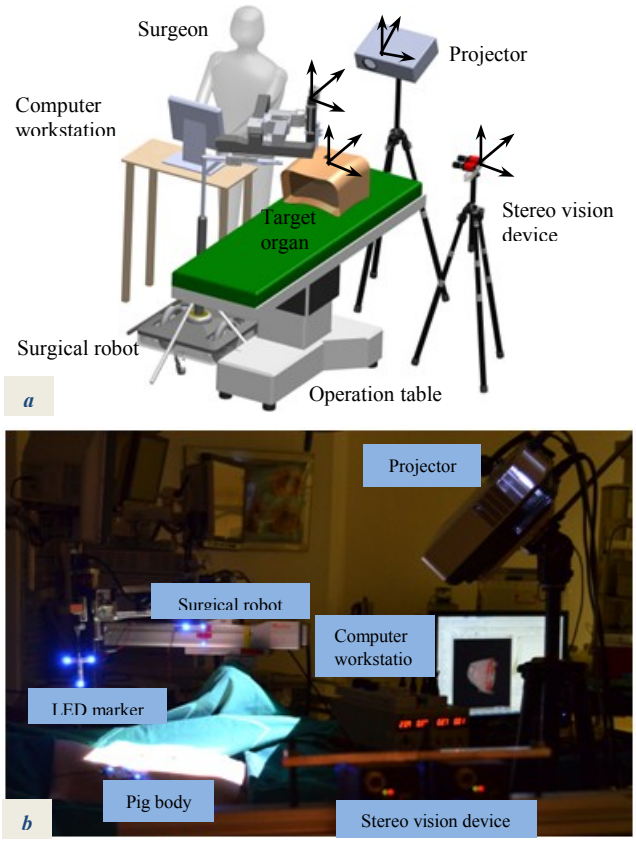

Fig. 1. System concept (a) and its setup in the operating room (b).

The system concept and its main components are shown in Fig. 1. It consists of a surgical robot, an LCD projector with resolution of 1024 ×768 (XGA), a stereo vision device with two industrial cameras and a computer workstation with quad-core processors, 12GB memory and a graphics card supporting OpenGL 3D. The surgical robot is specially designed and fabricated for the RFA treatment with multiple needle insertion. The computer workstation is the nucleus for data and surgical information processing such as medical image processing, surgical model construction and intensive calculation of massive matrices. The projector, stereo vision device and workstation constitute a projector-camera sub system which is used for construction of a spatial AR environment. The stereo vision device is also used for tracking RF needle insertion to provide a real-time feedback for robot navigation. In order to establish the relationship between the surgical robot and vision system, external fiducial markers are positioned on the patient skin, robot arms and RF needle's shaft for tracking and patent- model registration.

Software developed for this system includes modules of 3D model based surgical planning, calibration and construction of the projector-based AR environment, patient-model registration, surgeon's interactive supervisory guidance for planning update, vision-based tracking and model simulation based robot navigation.

III. Materials and Methods

A. Preoperative Planning

Surgical planning is applied with patient-specific medical data to generate the optimal ablation points, insertion points and insertion trajectories for the subsequent robot-assisted RF treatment. The medical data including pathological and anatomical information is acquired through patient CT scanning. The critical anatomical areas on the acquired CT images such as artery, hepatic vessels as well as the tumors are segmented. Anatomical models and tumor model are then constructed from the segmented profiles. A noninvasive marker frame attached on the patient's skin is also scanned for this preplanning. The marker frame is used to construct a coordinate system to register the patient model space to the world space. In addition, slight patient movement (e.g. breathing) can also be tracked by observing the markers with the stereo vision device.

In [4], we proposed a voxel-growing algorithm to construct ablation model for RFA treatment. This algorithm is specially designed for robot-assisted RFA solution in large tumor treatment to optimally complete the whole tumor ablation with minimal number of needle insertion. With the tumor and other anatomical structures visualized in 3D, an ablation model centered planning is adopted for the ablation treatment.

The ablation model is derived from tumor's 3D profile with a growing element. The element grows along the x, y and z axis to automatically generate ablation points within the tumor model's coordinate system. The growing element was assumed as a unit cube with a circumscribed sphere volume. A safety margin of 10 mm was considered in the ablation model in order to comply with the standard clinical practice [6]. The margin could be adjusted by selection of different growing element which resulted in different accuracy levels. With the generated ablation points and their relative position to tumor's peripheral anatomical structures, the insertion trajectories can be generated from the insertion points located on the patient skin to the ablation points (Fig. 2a). To ensure the anatomic structures are not harmed and the bones are avoided by the RF needle, the needle's position and orientation could be optimized by a gradient-based method [7]. Based on the above mathematic ablation model and insertion trajectories, surgeon's professional expertise and surgical experience are expected to examine the planning feasibility and its potential risks. In addition, the workspace of the surgical robot with respect to the preplanned needle placements is taken into consideration. It covers the entire tumor region and all the insertion trajectories avoiding the fiducial markers attached on the

patient (Fig. 2b).

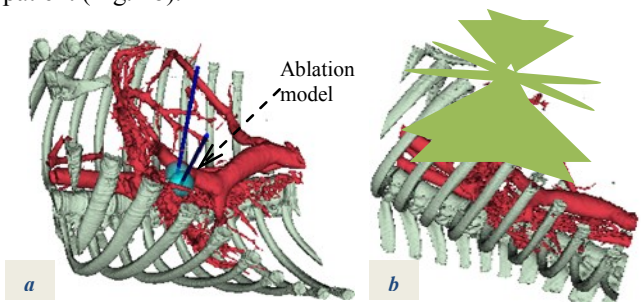

Fig. 2. (a) Ablation model planning based on anatomic models. (b) Path planning based on available workspace of surgical robot.

B. *Interactive Supervisory Guidance*

Patient's position and pose on the operation bed during surgery are not identical to that of during the CT scanning. Thus, the preoperative planning which is achieved based on the CT images cannot be immediately executed. In order to adapt the preoperative plan to for execution in a practical surgical setting, the projector-camera system provides the surgeon an interactive interface to offer his or her feedback. The projector-based AR display has advantages of direct interaction and open interface which enables surgeon to estimate surgical planning information directly from the patient body. However, its projection suffers geometric and radiometric distortion by a rough projection surface. Its display accuracy depends on matching accuracy of finding the pixel correspondence between the projector and cameras. Calibration with structured light pattern [8] may provide satisfied results for geometric and radiometric correction with this spatial AR display on an irregular surface. A piecewise linear based algorithm with chessboard pattern projection is another robust and practical method for calibration of projector-camera system [9]. With the calibration results, the preoperative surgical planning data can be directly visualized overlaying on the patient with satisfactory geometric and radiometric display.

Accurate display of the planning data on the specific position of the patient (skin) surface relies on patient-model registration. The patient-mode registration constructs spatial data mapping between the planning model space, patient space (constructed by the fiducial markers attached on the patient surface) and the world coordinate system. In this integrated surgical system, the projector-camera system is used not only for spatial AR display of the surgical information, but also as a spatial data acquisition system for patient-model registration. When the patient is settled on the operation bed for surgery, his surface data as well as position of the attached marker frame on his skin can be acquired by the projector-camera system [10]. By comparing these spatial data coordinates in two different data spaces: planning model space and patient space, the preoperative planning data is transferred to the current patient position. In this case, the surgical planning data, including preplanned ablation points, insertion points and the optimal trajectories can be mapped from the planning model space to the patient space and the world coordinate system.

With this direct AR interface, the surgeon can inspect the preoperative surgical planning directly from the current patient body. The position of the preplanned ablation model and the anatomic structure, especially of critical organs and vessels can be examined by the surgeon. Surgical risk of the execution of the preoperative plan in the real surgical environment can be estimated. Similarly, the preplanned surgical data with respect to the practical robot setup can be examined. With regard to the inappropriate planning data such as inappropriate insertion ports and trajectories, surgeon can interactively revise the corresponding preplanned data on the computer workstation and view the improved version on the AR interface immediately.

C. *Simulation-based Surgical Navigation*

Execution by the surgical robot performed after surgeon's approval of surgical plan, is monitored for each needle insertion through computer simulation using physics-based models in a computer-generated virtual environment. This virtual environment consists of surgical robot model, RF needle model, marker models and the patient model with preoperatively defined planning data. With stereoscopic vision system construction, the world coordinate system is established with its origin point centered at the principle point of the left camera [11]. Combination of mean-shift and Kalman filter algorithms [12] provides an effective and robust solution to vision based tracking of the LED makers for this surgical system. By measuring spatial coordinates of the LED markers attached on the robot arms and RF needle, the models' position in the virtual environment can be registered to their corresponding positions in the world coordinate system. Thus, the surgical planning data can be integrated into this virtual environment providing the surgeon with simulation of the robotic needle insertion during surgery.

By stereoscopic tracking of the fiducial markers attach to RF needle's shaft, the needle's spatial line vector in the world coordinate system is acquired. Its pose (angles relative to the axes of the marker frame) and position with respect to the maker frame attached on the patient body can then be derived. With patient-model registration matrix, $\mathbf{T}_{P\text{-}M}$, the current RF needle position with respect to the preplanned insertion points and the ablation points in the virtual environment can be obtained by:

$$\Delta p_i^{Vt} = {}^{V}\mathbf{T}_{W}\, p_i^{Wt} - {}^{V}\mathbf{T}_{W}\, {}^{W}\mathbf{T}_{P}\mathbf{T}_{P-M}^{-1}\, p_i^{Dt}, \qquad (1)$$

where p_i^{Wt} is the current position of needle's marker in the world coordinate system, p_i^{Dt} is the desired preplanned trajectory points in the planning model space. ${}^{V}\mathbf{T}_{W}$ and ${}^{W}\mathbf{T}_{P}$ are the transformation of coordinate system from the world space to the virtual environment and from the patient space to the world coordinate system respectively. The desired ablation point, p_{ai}^{Wt}, in the world coordinate system can be

derived from

$$p_{ai}^{Wt} = {}^{W}\mathbf{T}_{P}\,\mathbf{T}_{P-M}^{-1}\,{}^{M}\mathbf{T}_{Ma}\,p_{i}^{Mt} \quad (2)$$

where p_i^{Mt} is the i^{th} preplanned ablation point within the ablation model, and ${}^{M}\mathbf{T}_{Ma}$ is the transformation from ablation model space to the planning model space. When the RF needle approaches to the preplanned insertion points, simulation of spatial motion of robot arm execution and needle insertion provides kinematic input to the robot controller. The actual insertion trajectory is simulated and compared with the preplanned one to examine whether the actual trajectory is satisfactory.

D. Robotic System Design for Image-guided Surgery

Desired needle path planned by the surgeon is interpreted for computation of robotic trajectories in the joint domain. The robotic module in this study includes a manipulator mechanism together with its motion control software and a stereoscopic vision based coordinate system for execution of needle manipulation and insertion trajectories which has been developed specifically for robotic RFA application. Fig. 3 depicts the robotic manipulator proposed for the robotic system which is an expansion of our previous work [4].

The robotic arm is an 8 degree of freedom (DOF) serial manipulator comprising of 3 passive links and 5 motorized axles on a mobile base. It applies the concept of macro-micro manipulator for rapid deployment and fine placement of the needle. The first 3 passive links constitutes the main manipulator responsible for the deployment of the needle to an initial position. It is designed in a SCARA-like configuration which manipulates the sub-system in a cylindrical workspace. The 5-DOF sub-manipulator system located at the distal end is dedicated for precise needle insertions and is capable of dexterous manipulation for interventional procedures. The mobility of the joints is illustrated in Fig. 4. Its design facilitates programmable remote center of motion (RCM). RCM mechanism decouples rotation and translation motion of the surgical tools remotely from the robotic end effector [13], giving it the necessary dexterity required in transcutaneous interventional procedure. The entire robotic manipulator can be mounted on to a wheeled mobile base. Once the mobile base is at the desired position, vacuum suction locking mechanism at the base is activated to ground the manipulator's base firmly. In addition, the base is also equipped with supporting stands that can be deployed to stabilize the entire mechanism once in place. Alternatively, the manipulator can also be attached onto the rail of a standard surgical bed.

From the needle's initial position to the final ablation point, the robotic needle insertion follows a consistent insertion (insertion before reaching the insertion ports on the patient skin) and inconsistent insertion (insertion beneath the patient skin). During inconsistent insertion, deflection of the RF needle may occur, possibly causing the robot controller to calculate the instrument tip's position with invalid forward kinematics. A modified Jacobian-based controller which combines the feedback of stereoscopic vision and model simulation (Fig. 4) is used.

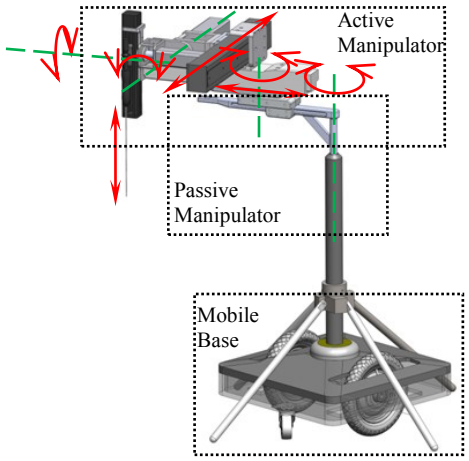

Fig. 3. Mobility of the robotic manipulator.

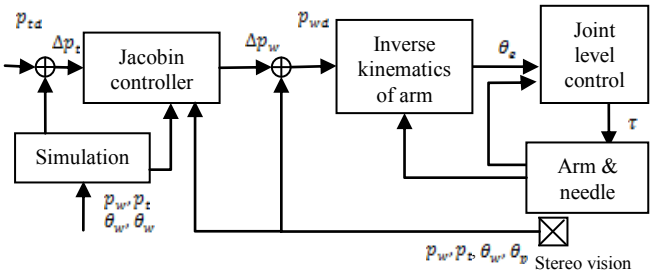

Fig. 4. Controller for the surgical robot system. $\boldsymbol{p_{td}}$ and $\boldsymbol{p_t}$ are the desired and current needle tip position respectively. $\Delta\boldsymbol{p_t}$ is the intended change in the needle tip position. $\boldsymbol{p_w}$ and $\boldsymbol{p_{wd}}$ are the desired and current needle shaft position respectively, $\Delta\boldsymbol{p_w}$ is the desired needle shaft motion. $\boldsymbol{\theta_g}$ is the joint angular position, and $\boldsymbol{\tau}$ is the motor torque.

IV. Experiments

Experiments were designed to assess the feasibility, consistency and accuracy of the robotic system. The system can be executed for operation in any ordinary operating theater with only the requirement of a few hours of set up time prior to the operation. The experiment methodology and procedure are discussed in this section.

A. Phantom model Tests

The proposed system was tested with its robotic and stereovision prototypical modules for its feasibility using a segment of *ex vivo* porcine liver with injected target tumor. The specimen was constrained in a SeaKem LE Agarose enclosure and underwent CT scanning. Fiducials were planted on the visible surface of the phantom model to create correspondence between CT image coordinates and operation workspace world coordinates. Before registration was carried out, electrical connectivity had to be ensured by providing physical contact between the liver in the phantom and grounding pad. Needle position and ablation of 1 cm security margin were subsequently performed. After

completing the ablation, the liver organ was removed from its enclosure and dissected to investigate the effect of ablation. Palpation was used to estimate the center of the ablated region before an incision was made. The charred area was then measured. The ablated boundary was observed to have circumscribed the implanted target uniformly, suggesting that the ablation was within the desired location.

To further test the accuracy of the needle trajectory, a solid phantom was constructed using SeaKem LE Agarose with modeling clay implanted within it to represent a tumor. Needle trajectories were executed with their planned path through the determined percutaneous entry points and into the respective tumors. The phantom was eventually sliced opened to examine the accuracy of the needle trajectories.

B. Animal Studies

Animal experiments were conducted to investigate the feasibility of the proposed mechanism. These studies were conducted in collaboration with surgeons and radiologists from National University Hospital, Singapore. It was carried out in the hospital under clinical setting, including the use of standard diagnostic imaging facilities. Clinical animal trials (IACUC Protocol Number 096/08) were carried out to validate the proposed mechanism. The experimental procedure is described as follows.

In order to create a phantom tumor in the live pig's liver, an experimented radio-opaque gel substance was injected into the liver to mimic a tumor target for ablation. CT scan was carried out to locate the position of the tumor. The medical image data obtained was presented in a visualization model on the planning interface. Segmentation of the tumor and periphery critical anatomic structures was then carried out for subsequent 3D model based prerogative surgical planning. Fig. 5a shows the resultant surgical planning based on the pig's specific 3D model which was reconstructed from the CT data set.

After the pig was placed on the operating table, a projection based AR display was overlaid on pig's belly, while the robot was registered to the surgical site. The AR display allowed the surgeon to examine the preplanning data directly from pig's body and provide his professional feedback for the planning. Projective geometric and radiometric corrections were achieved based on projector-camera calibration by serial projection of structured-light patterns on the pig's belly. With results of the patient-model registration, the preoperative plan was overlaid on the pig's belly. Fig. 5b shows this spatial AR based display on the pig's belly.

Based on the planned trajectory, the robotic manipulator first deployed the RF needle with the planned insertion pose in preparation for the planned point. A small incision on the percutaneous entry site was applied before insertion was carried out. This was to reduce the needle deflection and non-homogeneous deformation during the puncture phase. The simulated insertion trajectory was once again ascertained with the preoperative plan before generating the inputs to the robot controller for needle insertion. Upon completion of the needle insertion, the surgeon deployed the prongs at the tip of the RF needle to the desirable extent. RITA Radiofrequency Ablation System with real-time tissue monitoring was used to perform the ablation. Fig. 6 shows setup of robotic needle insertion during the animal experiment.

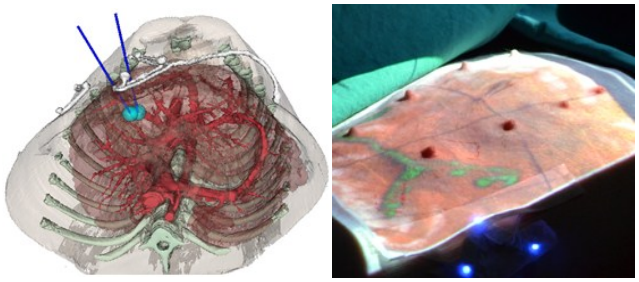

(a) (b)

Fig. 5. (a) Surgical planning based on pig's 3D model constructed from the CT data set. (b) AR display of planning data on the pig's belly.

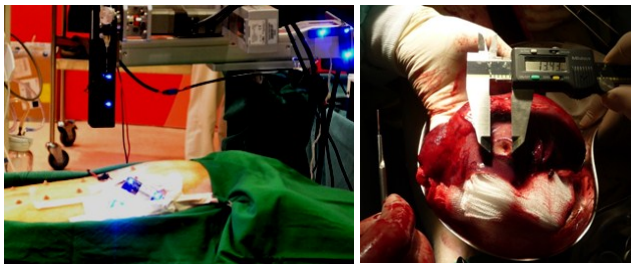

(a) (b)

Fig. 6. (a) Surgical navigation using stereoscopic tracking and simulation. (b) Ablation region examination and measurement.

After the ablation procedure, a post ablation MRI scanning was performed to examine ablated tumor tissue. The surgeon examined the image and assessed the outcome of the ablation. The portion of tumor which the ablation missed can be identified in the image. At the end of the surgery the liver was harvested for evaluation (Fig. 6b).

V. Results and Discussion

Evaluation of the accuracy and precision of insertion trajectory takes into account the linear and angular errors. A series of spatial positions of markers which represent the actual insertion trajectory were acquired while the robot executed a given trajectory. The registration error of the marker's positions between the camera coordinate system and the model planning coordinate system has a mean value of 1.27 mm in one axis of the fiducial frame. In 3D space, the mean linear displacement error can be approximated as 2.2 mm. The average angular error registered for the same set of trajectory was 0.006^{o}. The standard deviation of the linear displacement registered was 1.44 mm.

Experiments on phantoms suggested a mean targeting error of 3.92 mm at the incision site and 4.01 mm at the tumor. This is obtained by measuring the needle tract

indented within the phantom from the desired point of entry and target respectively. From the post ablation MR image, the ablation region was found to have encompassed the entire phantom tumor. Actual targeting error for the animal experiment was 5.33 mm. This was verified when the tumor was harvested and examined. The maximum dimension of the residual tumor from the ablation region is 7.26 mm. Standard security margin was intentionally not applied so that the ideal ablation volume is exactly equivalent to the encompassing sphere computed by the planning software. In surgery, 10 mm of security margin is ablated in addition to the estimated volume required to encompass the targeted tissue region. The measurement of diameter of ablation regions around the ablation points, which are 20.80 mm and 21.06 mm compared with the expected 20.00 mm, indicated that whole tumor regions were ablated. The radiofrequency conductivity in non-homogenous tissue may also contribute to this increased ablation regions.

The feasibility of the system is demonstrated by the animal studies. The experimental data has yielded promising results in terms of accuracy and precision, supporting the feasibility of the proposed system. Feedback from clinicians has been generally positive especially in the relevance of its application. The proposed methodology has great potential to be extended to a highly robust system with enhanced or existing hardware modules. This however requires an extensive period of engineering analysis and tests to ensure its robustness and compliance with existing clinical standard. The current robustness of the system against intraoperative uncertainties can be further improved. For instance, the issue of compensation for tissue deformation should be addressed in future studies. This is however beyond our scope as the incorporation of any deformation prediction module is technically trivial. The real challenge is on developing an accurate tool tissue interactive model. This is an issue which we are working on extensively [14].

VI. Conclusion

A system for interactive planning and monitoring in robot transcutaneous interventional procedure is proposed and demonstrated in this study. The proposed system is tested for its accuracy, precision and feasibility for actual clinical procedure. The study supported the potential of its development into a one-stop solution for interventional therapy covering preoperative plan to intraoperative execution. This solution is promising in overcoming current technological limitations and practical constrains of real-time medical imaging in transcutaneous ablation therapy.

Acknowledgment

The authors would like to thank Liangjing Yang for his expertise and support on surgical robot design and setup, Bingnan Li and Gang Wang for their contribution to the medical image processing system.

References

[1] S. Garrean, J. Hering, A. Saied, W. S. Helton, and N. J. Espat, "Radiofrequency ablation of primary and metastatic liver tumors: a critical review of the literature," *The American Journal of Surgery*, vol. 195, pp. 508-520, Apr. 2008.

[2] R. Rai and D. Manas, "Radiofrequency ablation of liver tumours," *Surgery (Oxford)*, vol. 21, pp. iii-vi, Aug. 2003.

[3] M. Nakamoto, K. Nakada, Y. Sato, K. Konishi, M. Hashizume, and S. Tamura, "Intraoperative magnetic tracker calibration using a magneto-optic hybrid tracker for 3-d ultrasound-based navigation in laparoscopic surgery, " *IEEE Trans. Medical Imaging*, vol. 27, pp. 225-270, Feb. 2008.

[4] L. Yang, R. Wen, J. Qin, C.K. Chui, K. B. Lim, and S. K. Y. Chang, "A robotic system for overlapping radiofrequency ablation in large tumor treatment," *IEEE/ASME Trans. Mechatronics*, vol.15, no.6, pp.887-897, Dec. 2010.

[5] G. Fichtinger, A. Deguet, K. Masamune, E. Balogh, G.S. Fischer, H. Mathieu, R.H. Taylor, S.J. Zinreich and L.M Fayad, "Image overlay guidance for needle insertion in CT scanner," *IEEE Trans. Biomedical Engineering,* vol.52, no.8, pp.1415-1424, Aug. 2005.

[6] M. H. Chen, W. Yang, K. Yan, M. W. Zou, L. Solbiati, J. B. Liu, and Y. Dai, "Large liver tumors: Protocol for radiofrequency ablation and its clinical application in 110 patients—mathematic model, overlapping mode, and electrode placement process," *Radiology*, vol. 232, pp. 260–271, Jul. 2004.

[7] S. Haase, P. Süss, J. Schwientek, K.Teichert, and T. Preusser, " Radiofrequency ablation planning: An application of semi-infinite modeling techniques," *European Journal of Operational Research*, vol. 218, no. 3, pp. 856-864, May 2012.

[8] A. Griesser and L. Van Gool, "Automatic interactive calibration of multi-projector-camera systems," in *Proc. IEEE. Conf. Computer Vision and Pattern Recognition Workshop(CVPRW)*, 2006, pp.8-8.

[9] R. Wen, L. Yang, C. K, Chui, K. B. Lim, and S. Chang, "Intraoperative visual guidance and control interface for augmented reality robotic surgery," in *Proc. IEEE Int. Conf. Control and Automation (ICCA),* 2010, pp. 947 - 952.

[10] R. Krempien, H. Hoppe, L.Kahrs, S. Daeuber, O. Schorr, G. Eggers, M.Bischof, M.W. Munter, J.Debus and W. Harms "Projector-based augmented reality for intuitive intraoperative guidance in image-guided 3d interstitial brachytherapy," *International Journal of Radiation Oncology*Biology*Physics*, vol. 70, pp. 944-952, Mar. 2008.

[11] R. Wen, C. K. Chui, and K. B. Lim, "Intraoperative visual guidance and control interface for augmented reality robotic surgery," *in Augmented Reality-Some Emerging Application Areas*, InTech, 2010, pp.191-208.

[12] N. Peng, J. Yang, and E. Liu, "Model update mechanism for mean-shift tracking," *Journal of Systems Engineering and Electronics*, vol. 16, pp. 52 - 57, Mar. 2005.

[13] L. Yang, C. B. Chng, C. K. Chui, and D. Lau, "Model-based Design Analysis for Programmable Remote Center of Motion in Minimally Invasive Surgery " in *4th IEEE international Conference on Robotics, Automation and Mechatronics*, 2010, pp 84-89.

[14] W.H. Huang, C.K. Chui, E. Kobayashi, S. H. Teoh, and S. Chang, "Multi-scale model for investigating the electrical properties and mechanical properties of liver tissue undergoing ablation," in *International Journal of Computer Assisted Radiology and Surgery*, 2011, pp. 601-607.